

MULTICOMPONENT CHIRP DEMODULATION USING DISCRETE FRACTIONAL FOURIER ANALYSIS

Lakshmikanth Reddy S, Balu Santhanam and Majeed Hayat

Department of E.C.E.
University of New Mexico, Albuquerque, NM 87131
Email: bsanthan,hayat@ece.unm.edu

ABSTRACT

The multicomponent chirp model finds numerous applications in biomedical signal processing, radar problems, and in the modeling of biological waveforms such as bat and whale echolocation signals. The problem of demodulating these signals is straight-forward when the components are distinct, however, when the components overlap spectrally or when one of the components is stronger than the others existing multicomponent demodulation algorithms run into singularity problems and are unable to effect signal separation and demodulation. In this paper, we present a method of multicomponent chirp demodulation using the recently introduced multi angle-centered discrete fractional fourier transform. We specifically demonstrate that the proposed algorithm is effective in the aforementioned difficult situations where other algorithms fail.

1. INTRODUCTION

One encounters multicomponent chirp signals in several applications such as: (a) biomedical problems where the second heart beat sound is modeled using chirps [7], (b) communication systems where relative motion between transmitter and receiver manifests as a Doppler shift, (c) multiple target tracking problem in radar systems, and when dealing with several real-world signals such as bat and whale echolocation signals [2]. If the components are well separated spectrally and distinct then traditional bandpass filtering can be used to isolate the components followed by monocomponent demodulation. However, when the components overlap spectrally or when one of the components is much stronger than the others then the existing multicomponent demodulation algorithms encounter singularity problems and are unable to accomplish this task [5].

In recent years, there has been significant interest in the area of *discrete fractional Fourier analysis* (DFRFT) because of the capability of the underlying transform to concentrate linear chirp signals in a few coefficients [1, 3]. Empirical expressions that relate the chirp rate and center frequency of each component to the coordinates of the peaks of the multiangle version of centered discrete fractional Fourier transform (MA-CDFRFT) were discussed in [1]. The MA-CDFRFT has also recently been used to define

This work was supported by the AFRO and Optimetrics Inc., Ohio, through subcontract agreement 23654

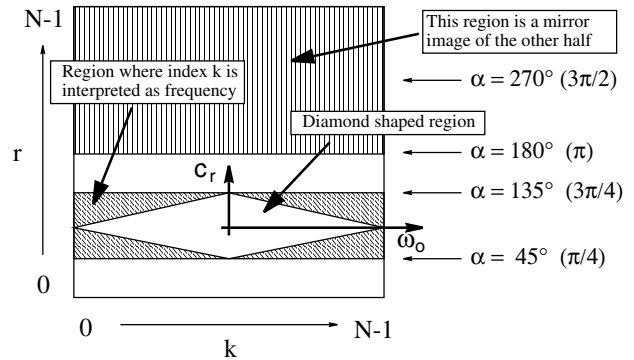


Figure 1: Map of $\mathbf{X}_k[r]$ depicting the region where the index k is interpreted as frequency and the diamond shaped region where no aliasing occurs.

a modified spectrogram that is based on the multicomponent chirp model and more suited for the analysis of chirp signals [2].

In this paper, we present a framework for multicomponent chirp demodulation that uses the MA-CDFRFT and the associated chirp-frequency representation [3]. Through simulations we demonstrate the validity of the approach specifically in the three challenging cases where: (a) the carrier frequencies of the components are identical, (b) the IF's of the components intersect, (c) the relative power of one component over the other is very large.

2. MULTICOMPONENT CHIRP MODEL

Multicomponent linear chirp signals are signals of the form:

$$x[n] = \sum_{i=1}^K A_i \cos \left(\int_0^n \Omega_i[m] dm + \theta_o \right), \quad (1)$$

where the *instantaneous frequency* (IF) of the i^{th} component is given by

$$\omega_i[n] = \omega_{ci} + c_{ri} \left(n - \frac{N-1}{2} \right), \quad 0 \leq n \leq N-1, \quad (2)$$

and ω_{ci}, c_{ri} are the carrier frequency and chirp rate of the i^{th} component. For the sake of brevity, we adopt the param-

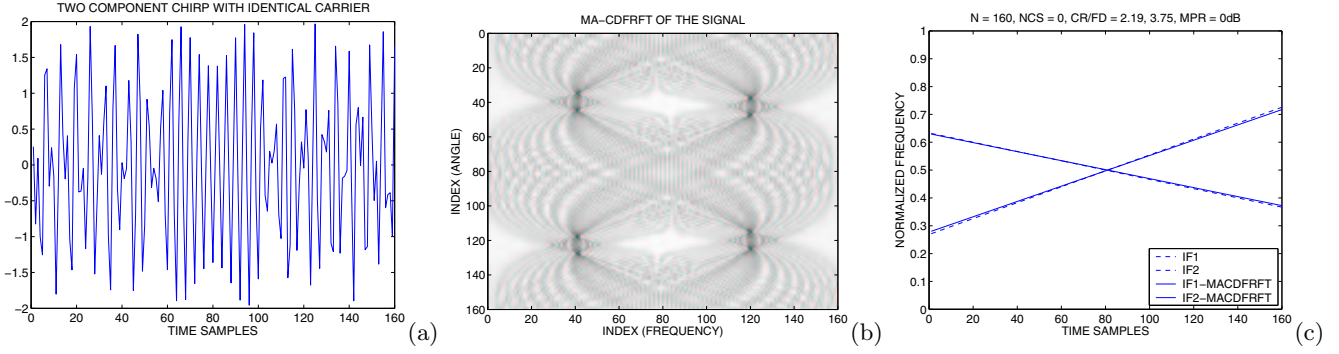


Figure 2: Cochannel problem: (a) composite linear-FM signal, (b) magnitude of the corresponding MA-CDFRFT, (c) estimated IF's using the MA-CDFRFT approach, where actual IF's are in solid lines and estimates are in dashed lines.

eters and performance measures discussed in [5] for comparing the performance of the various multicomponent demodulation algorithms. Specifically we will use the *normalized carrier separation* (NCS) parameter as a measure of spectral separation and the *mean power ratio* (MPR) parameter to measure the relative power between components. Towards avoiding aliasing, we restrict the chirp rate of each component to be small in comparison to the respective carrier frequency, i.e., we are assuming that the components have large *carrier-frequency-to-information bandwidth* (CR/IB) and *carrier-frequency-to-frequency deviation* (CR/FD) ratios [5].

A complete overview of different multicomponent AM-FM demodulation algorithms, comparison of the performance of the different approaches, discussion of their relative merits and disadvantages, and a discussion of the problems encountered by these algorithms in the above mentioned difficult situations has been carried out in [5].

3. DISCRETE FRACTIONAL FOURIER ANALYSIS PRIMER

The *discrete fractional Fourier transform* (DFRFT) as defined in [1, 3] is given by the fractional power of the DFT matrix:

$$\mathbf{X}_\alpha = \mathbf{A}_\alpha \mathbf{x} = \mathbf{W}^{\frac{2\alpha}{\pi}} \mathbf{x},$$

where \mathbf{W} is the traditional DFT matrix. The motivation for this transform was the time-frequency analysis of signals that had time-frequency coupling, such as linear chirps. The *centered DFRFT* (CDFRFT) based on the Grunbaum commuting matrix and the centered version of the DFT is defined as [1, 3]:

$$\mathbf{X}_\alpha = \mathbf{V}_G \mathbf{A}^{\frac{2\alpha}{\pi}} \mathbf{V}_G^T \mathbf{x}, \quad (3)$$

where \mathbf{V}_G is the matrix of eigenvectors obtained from the Grunbaum commuting matrix and its columns serve as discrete counterparts of Gauss-Hermite functions.

It was shown in [1] that this transform has the ability to concentrate linear chirps in a few coefficients. Specifically it was shown that we obtain an impulse-like transform similar to what the DFT produces for sinusoids if we choose the

appropriate angle α that corresponds to the chirp rate of the signal according to the empirical relation

$$\mathbf{c}_r = 2 \frac{\tan(\alpha_p - \pi/2)}{N} + 1.41 \frac{(\alpha_p - \pi/2)}{N} \quad (4)$$

where \mathbf{c}_r is the chirp rate defined as the coefficient of the quadratic term of the phase, and α_p is the angle of the CDFRFT for which we obtain the peak. The center frequency of the chirp can also be related to the angular parameter via:

$$\omega_o = \omega_p + (\alpha - \pi/2)^3, \quad (5)$$

where ω_p is the location of the peak along the frequency axis. The MA-CDFRFT is obtained by computing the CDFRFT for the set of uniformly spaced angles $\alpha_r = \frac{2\pi r}{N}$, $r = 0, 1, \dots, N-1$, using the method developed in [3].

The MA-CDFRFT is a matrix, $\mathbf{X}_k[r]$, that corresponds to a time-frequency representation in which time and frequency share the same axis (index k), and depending on the value of α we interpret the index as time or frequency. Fig. 1 shows the representation of the matrix $\mathbf{X}_k[r]$. The index r is interpreted as chirp rate and index k is interpreted as center frequency. The proposed chirp demodulation algorithm will make use of the coordinates of the maxima of the MA-CDFRFT in the chirp-rate frequency representation to perform multicomponent chirp demodulation.

When computing the MA-CDFRFT of a complex sinusoidal signal we always obtain two peaks, one in the lower half and the other in the upper half of $\mathbf{X}_k[r]$, and if the signal has a constant frequency, the peaks will be located exactly at the rows corresponding to angles $\alpha = 90^\circ$, 270° that correspond to the centered DFT (CDFT), and its inverse. With a real signal we obtain four peaks due to the relevant symmetries. A signal with a chirp rate different than zero will produce peaks at angles different than 90° and 270° , and they will be above or below those values depending on the sign of the chirp rate. As described in Fig. 1, the chirp-rate and center-frequency need to lie within the diamond shaped region in the chirp-rate vs. frequency plane to avoid aliasing.

In recent work [2], the MA-CDFRFT has been used to define a modified spectrogram that produces sharper features. The essential feature of the modified spectrogram is

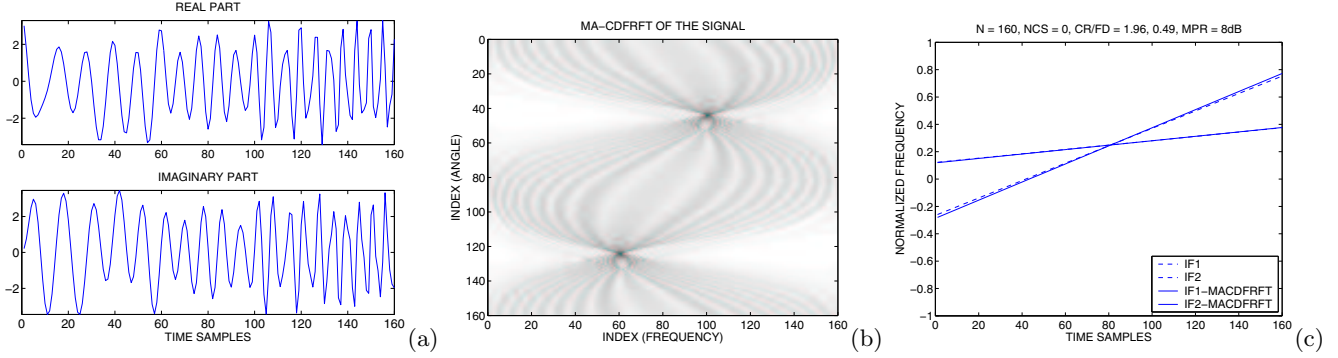


Figure 3: Effect of MPR: (a) real and imaginary part of the signal (b) magnitude of the corresponding MA-CDFRFT, (c) estimated IF's using MA-CDFRFT, where actual IF's are in solid lines and estimates are in dashed lines.

that it is based on the multicomponent chirp model rather than a multicomponent sinusoidal model and was shown to be more effective at representing chirps.

4. SIMULATION RESULTS

In these simulations, we will demonstrate the efficacy of the proposed approach specifically in three situations: (a) for identical carrier frequencies, (b) for large relative power ratios, (c) when the IF tracks of the components intersect. Existing multicomponent demodulations algorithms completely fail in these situations.

4.1. The cochannel problem

When the components of the multicomponent chirp are well separated spectrally and distinct then the problem of demodulation is straight-forward and simple bandpass filtering followed by monocomponent demodulation can accomplish the task. However, when there is significant spectral overlap then the components are not distinct. This situation is called the *cochannel problem* and occurs in communication systems, when several users of interest are present in the same channel [5]. This situation corresponds to the case where the NCS parameters is less than 1.

The proposed MA-CDFRFT based approach is able to accomplish demodulation even when the components have the same carrier frequency. Consider the two component sinusoidal chirp example, where $NCS = 0$, $CR/FD = 2.19, 3.75$ and $MPR = 0dB$. Fig. 2(a) shows the real chirp signal, Fig. 2(b) shows the the magnitude of the MA-CDFRFT, Fig. 2(c) depicts the estimated IF's using the MA-CDFRFT and the original IF's. The first component has a positive chirp rate $\frac{\pi}{350}$ and the second component has a negative chirp rate $\frac{\pi}{600}$. We can observe that there are actually four maxima corresponding to each chirp signal. The x coordinates of the maxima is at $k=40$ which corresponds to the center frequency = $\frac{40.2\pi}{160}$. The y coordinate of the maxima are at $r = 35$ and 50 . Upon application of Eq. (4), the corresponding chirp rate estimates are 0.0051 and 0.0086. The PASSED algorithm developed in [5] can also in principle perform multicomponent chirp demodulation in the cochannel

setting, however, this algorithm requires periodic extension of the components.

4.2. The near-far problem

If some components of the composite chirp signal are much stronger than the others then this situation will manifest as a singularity problem in the eventual demodulation of the weaker component. This situation that occurs in wireless communication systems is referred to as the *near-far problem* or the *capture effect* and translates to a large value for the MPR parameter. Specifically let us look at the two-component complex chirp signal in Fig. 3(a), where $NCS = 0$, $CR/FD = 1.96, 0.49$ and $MPR = 8dB$. Fig. 3(b) depicts the MA-CDFRFT corresponding to the composite signal where we can still observe the peak corresponding to the weaker chirp.

4.3. Case of the intersecting IF Tracks

Consider the two component chirp example in Fig. 5(a) where $NCS = 0$, $CR/FD = 2.19, 3.75$ and $MPR = 0dB$. In the above example, the component IF's cross-over. This parameter setting is not only indicative of significant spectral overlap between the components but also challenging from the perspective of frequency assignment at the cross-over point. In Fig. 5(b) we can observe the maxima corresponding to the chirp rates and center frequencies even though the IF's cross-over. Existing multicomponent AM-FM demodulation algorithms are at a loss to perform frequency assignment at the cross-over point to either component and prior information is needed to allocate this frequency. Specifically in this situation the *Hankel Rank Reduction* (HRR) [4] algorithm encounters state flipping, the underlying state model becomes unobservable, and the algorithm is unable to accomplish the demodulation task when the IF's cross-over [5]. Fig. 5(c) depicts the estimated IF's of both methods and the flipping of the IF estimates at the cross-over point.

4.4. Two component chirp in noise

An example of the MA-CDFRFT applied to a noisy two component chirp signal is shown in Fig. 6. Fig. 6(a) is

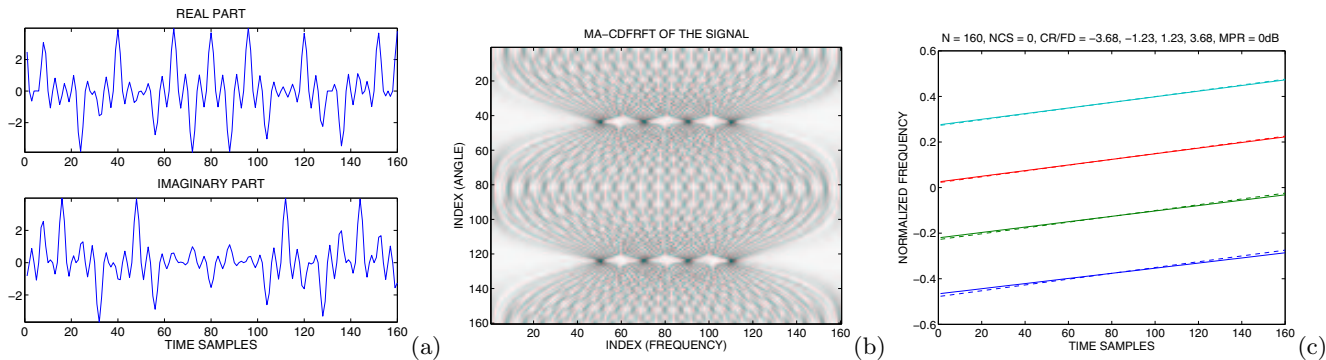


Figure 4: Four Component Chirp: (a) real and imaginary part of the signal (b) magnitude of the corresponding MA-CDFRFT, (c) estimated IF's using MA-CDFRFT, where actual IF's are in solid lines and estimates are in dashed lines.

the MA-CDFRFT of the noiseless signal. Fig. 6(b) is the MA-CDFRFT of the signal with a SNR of -8 dB. Although there is significant noise in the second image, the peaks corresponding to the chirps are still clearly visible. The efficiency of the proposed multicomponent chirp demodulation approach in AWGN is directly related to the efficiency of the constituent center-frequency and chirp-rate estimators. Fig. 7 (a,b) depict the normalized MSE of the MA-CDFRFT approach in comparison to the CRLB for monocomponent chirp demodulation in AWGN [6].

From the MSE curves, we can make some central observations: (a) carrier frequency estimation is about 20-25 dB more robust in comparison to chirp-rate estimation, (b) a SNR threshold of around -5 dB is needed for the proposed approach, (c) resolution limitations of the FFT employed in the MA-CDFRFT approach are reflected in the induced error floor, (d) increasing the FFT size, lowers this error floor at the expense of computational complexity.

4.5. Multicomponent Chirps

Consider the four component chirp signal example in Fig. 4(a), where $NCS = 0$, $CR/FD = -4.9, -2.45, 0.2, 2.45$ and $MPR = 0\text{dB}$. Fig. 4(b) depicts the MA-CDFRFT corresponding to the composite signal, Fig. 4(c) depicts the estimated IF's using the MA-CDFRFT and the original IF's. The proposed MA-CDFRFT approach is able to detect the peaks that correspond to the four different components. Unlike the PASED algorithm, we do not have to worry about pair-wise interactions or higher-order interactions between the components. Furthermore, note that unlike the energy-operator based PASED algorithm that requires large CR/FD ratios, the proposed approach works well in baseband parameter settings also.

5. CONCLUSIONS

In this paper, we have introduced a framework for multicomponent chirp demodulation based on the multiangle version of the DFRFT and the associated chirp-rate frequency representation. We have shown through simulations that this framework is particularly effective in dealing with the difficult cases where the components of the

multicomponent chirp signal overlap spectrally and are not longer distinct, or when one of the components is significantly stronger than the other, or when the component IF tracks cross-over. The proposed approach is able to accommodate both a baseband and bandpass signal model. The simulations presented demonstrate the effectiveness of this approach in dealing with these difficult situations where all existing demodulation algorithms are known to develop singularity problems and fail.

REFERENCES

- [1] J. G. Vargas-Rubio and B. Santhanam, "The Centered Discrete Fractional Fourier Transform and Linear Chirp Signals," *Proc. of 11th IEEE DSP Workshop*, pp. 163 - 167, 2004.
- [2] J. G. Vargas-Rubio and B. Santhanam, "An Improved Spectrogram Using the Multiangle Centered Discrete Fractional Fourier Transform," *Proc. of ICASSP-05*, Vol.IV, pp. 505-508, Mar. 2005.
- [3] J. G. Vargas-Rubio and B. Santhanam, "On the Multiangle Centered Discrete Fractional Fourier Transform," *IEEE Signal Proc. letters*, Vol. 12, No. 4, pp. 273-276, Apr. 2005.
- [4] C. L. Dimonte and K. S. Arun, "Tracking the frequencies of superimposed time-varying harmonics," *Proc. of ICASSP-90*, pp. 2356-2362, 1990.
- [5] Balu Santhanam and Petros Maragos, "Multicomponent AM-FM Signal Separation and Demodulation Via Periodicity Based Algebraic Separation and Energy Based Demodulation," *IEEE Trans. Communication*, Vol. 48, No. 473-490, 2000.
- [6] R. M. Liang and K. S. Arun, "Parameter Estimation for Superimposed Chirp Signals," *Proc. of ICASSP-92*, Vol. 5, pp. 273-276, 1992.
- [7] J. Xu, L. Durand, P. Pibarot, "Nonlinear Transient Chirp Signal Modeling of Aortic and Pulmonary Components of the Second Heart Beat Sound," *IEEE Trans. on Biomed. Engr.*, Vol. 47, No. 10, pp. 1328-1335, 2000.

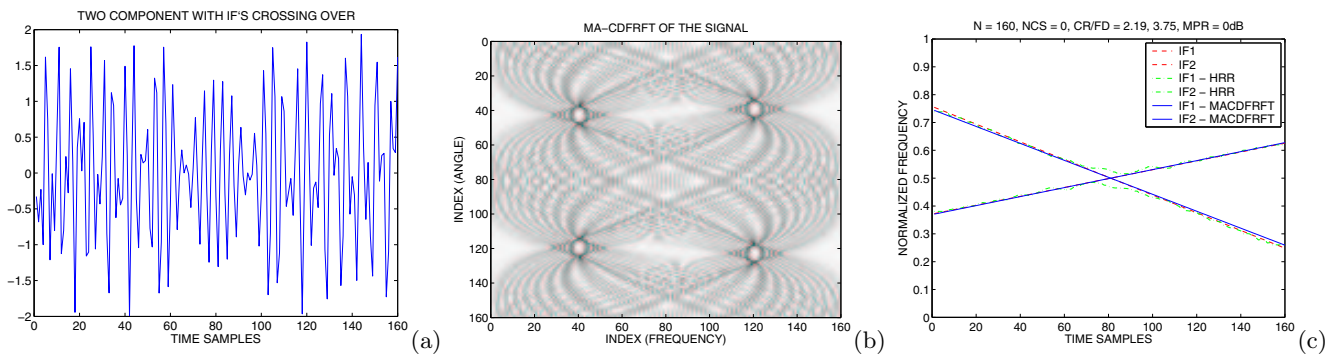


Figure 5: IF's crossing over: (a) composite linear-FM signal (b) magnitude of the corresponding MA-CDFRFT (c) comparison of frequency demodulation results using HRR method and MA-CDFRFT method, where actual IF's are in solid lines and estimates are in dashed lines.

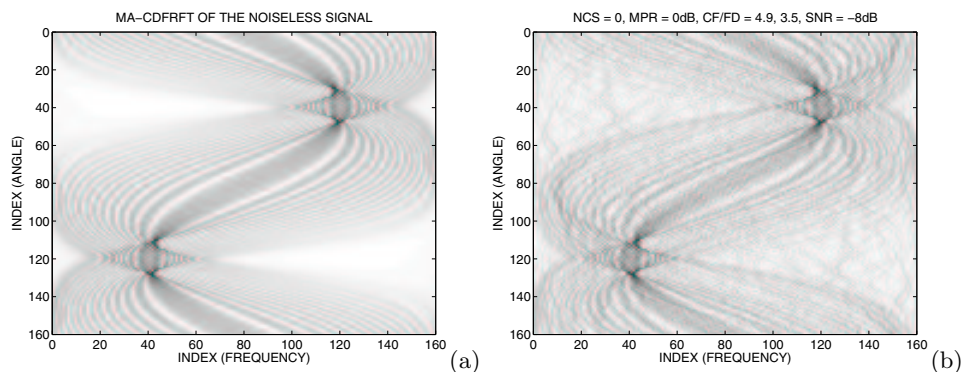


Figure 6: Chirp demodulation in AWGN: (a) MA-CDFRFT magnitude of the noiseless signal and (b) the corresponding MA-CDFRFT magnitude for a SNR of -8dB

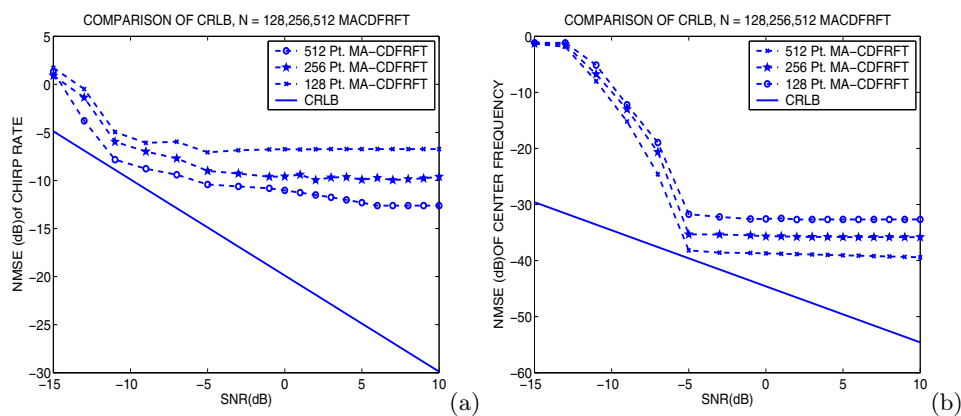


Figure 7: Performance evaluation: (a,b) comparison of the normalized MSE of the center-frequency and chirp-rate estimates of the proposed MA-CDFRFT approach in AWGN and the corresponding CRLB.